Highly Sensitive Focus Monitoring on Production Wafer by Scatterometry Measurements for 90/65-nm Node Devices

Toshihide Kawachi, Hidekimi Fudo, Yoshio Iwata, Shunichi Matsumoto, Hideaki Sasazawa, and Tadayoshi Mori

***Abstract*—RENESAS factories are starting to use scatterometry for inline focus measurement. This paper presents the development of the method used for nondestructive, high accuracy, and high-speed focus measurement on production wafers. Focus change results in a subtle variation of the photoresist shape, and this phenomenon is parameterized by using a new eight-layer model. Partial least squares regression methods are used to calculate focus from scatterometry measurement results. The measurement error for a focus variation of 0.1 μm is within 30 nm. This method enables the focus offset to be corrected more frequently without increasing the aligner machine downtime and reduces the depth of focus required because of aligner fluctuation. With it, we will be able to get sufficient focus margins for mass production of devices beyond the 65-nm-node devices.**

***Index Terms*—Focusing, photolithography, resists, scatterometry.**

I. Introduction

DESIGN rules for semiconductor devices are continually decreasing as shown in ITRS road maps. We can see in Table I that a 38-nm gate length will be required in high-end MPUs by 2008 and that the gate length will continue to decrease by 10% or more each year [1].

Photolithography reduces design rules by continuously developing technology increasing micropattern resolution technology. The pattern resolution R in projection printing is governed by the Rayleigh criterion

$$\mathrm{R} = \mathrm{k}_1 \left(\frac{\lambda}{\mathrm{NA}} \right) \quad (1)$$

where λ is the wavelength of the light source, NA is the numerical aperture of the lens, and the factor k_1 reflects the effects of various kinds of resolution enhancement techniques that are widely used today: modified illumination, correction for the optical proximity effect, phase-shift masks, and advanced photoresist processes. Resolution can be enhanced by using light sources with shorter wavelengths, like the 193-nm ArF excimer lasers that have become mainstream technology, and by increasing the numerical aperture (NA). The NA of the dry type of ArF scanner has already reached 0.93, and future immersion-type scanners will provide an NA greater than 1.30. Since the depth of focus (DOF) of a lens is inversely proportional to the NA, the rapid rise of NA in recent years has caused a rapid decrease of DOF and thus of the focus margins in the exposure process. As shown in Fig. 1, the required DOF in mass production lithography process is determined by the DOF due to the variation of each component of the exposure equipment, that is, by wafer flatness, wafer chuck flatness, reticle flatness, and exposure equipment stability. The focus margin of each layer's exposure process is defined as the "production focus margin," and mass production is difficult when the production focus margin is less than required DOF.

Generally, the required DOF decreases with each new design rule. This is due to the year-by-year improvement of the exposure equipment performance and the flatness of various component parts. When the node size is less than 90 nm, however, the production focus margin decreases faster than the required DOF. As a result, we sometimes cannot obtain a production focus margin sufficient for advanced devices. Equipment stability will become more important, because it is difficult for device makers to improve the flatness of each component. Alignment equipment is therefore used to periodically adjust focus offset according to focus measurements made with special QC wafers. This procedure decreases productivity because the time spent on the QC measurements cannot be used for production. Focus measurements are therefore made only a few times per month. If we had a high-precision focus measurement technique that we could use with the production wafers, we would be able to adjust the focus offset daily.

Several inline focus measurement techniques using special marks have been proposed [2]–[4], but with them it is difficult to detect the focus variation of the production pattern itself. A new focus measurement technique tried to solve this problem by using cross-sectional scanning electron microscopy (X-SEM) to observe the profile of a line-and-space photoresist (PR) pattern whose shape is the same as that of the production pattern, but PR profile measurement is difficult on production wafers. What we need instead is a 3-D pattern measurement tool which can rapidly measure the PR profile nondestructively and accurately. Although scatterometry is such a tool and should be useful for detecting PR profile fluctuation on production wafers, it has not yet been used to measure small variations of PR profile.

Manuscript received February 15, 2007; revised May 24, 2007.

T. Kawachi, H. Fudo, and Y. Iawata are with Renesas Technology Corporation, Ibaraki 312-8504, Japan (e-mail: kawachi.toshihide@renesas.com; fudo.hidekimi@renesas.com; iwata.yoshio@renesas.com).

S. Matsumoto and H. Sasazawa are with Hitachi, Limited, Kanagawa 244-0817, Japan (e-mail: shunichi.matsumoto.sz@hitachi.com; sasazawa.hideaki@gm.perl.hitachi.co.jp).

T. Mori is with Nanometrics Japan, Limited, Tokyo 141-0031, Japan (e-mail: tmori@nanometrics.co.jp).

Color versions of some of the figures in this paper are available online at http://ieeexplore.ieee.org.

Digital Object Identifier 10.1109/TSM.2007.901831

0894-6507/$25.00 © 2007 IEEE

TABLE I
LITHOGRAPHY TECHNOLOGY REQUIREMENTS (FROM ITRS ROADMAP 2006 UP DATE) [1]

Year of Production	*2005*	*2006*	*2007*	*2008*	*2009*	*2010*	*2011*	*2012*	*2013*
MPU									
MPU/ASIC Metal 1 (M1) ½ pitch (nm)	90	78	68	59	52	45	40	36	32
MPU gate in resist (nm)	54	48	42	38	34	30	27	24	21
*MPU physical gate length (nm) **	32	28	25	23	20	18	16	14	13
Contact in resist (nm)	111	97	84	73	64	56	50	44	39
Contact after etch (nm)	101	88	77	67	58	51	45	40	36
*Gate CD control (3 sigma) (nm) [B] ***	◆3.3	◆2.9	2.6	2.3	2.1	1.9	1.7	1.5	1.3
MPU/ASIC Metal 1 (M1) ½ pitch (nm)	90	78	68	59	52	45	40	36	32

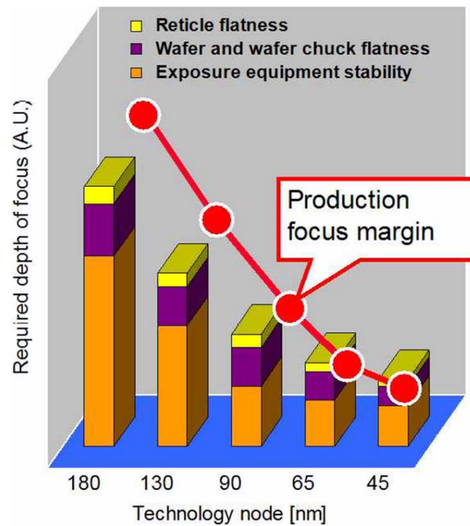

Fig. 1. Required depth of focus and focus margin for various technology nodes.

This paper presents our new technique using scatterometry for inline focus measurement. In Section II, we study the possibility of detailed PR profile measurement by this tool. A multilayer scatterometry model is developed and realizes the measurement of slight variation of PR profile by focus fluctuation. In Section III, we study the analysis technique of extracting the focus fluctuation from PR profile measurement results and derive the focus prediction formula. We carried out the accuracy evaluation of focus measurement results and compared with conventional method. We summarize our conclusion in Section IV.

II. MEASUREMENT TECHNIQUE

Focus fluctuation changes the PR profile as shown in Fig. 2, where we can see that the upper portion of the profile becomes wider when the fluctuation is positive and narrower when the fluctuation is negative.

The dimensions of a periodic 3-D pattern on focus exposure matrix (FEM) wafers are measured nondestructively by scatterometry. The measurement target is a 50-μm-square area in a grating pattern comprising 110-nm lines separated by 250-nm spaces, and the focus and exposure dose are changed at each shot.

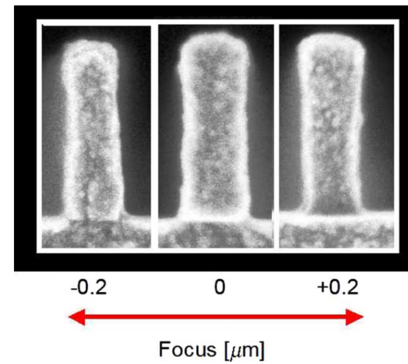

Fig. 2. Photoresist profiles due to positive and negative fluctuation of focus.

A. System Configuration

Fig. 3 shows the configuration of measurement system. Input light passes through the polarizer and is incident normal to the surface of the grating sample. Polarizer rotation is controlled by the system so that the polarization of the incident light can be set either parallel or orthogonal to the grating lines. For measurement analysis the system uses zeroth-order diffracted light from the grating sample, and it is designed to suppress high-order diffraction of reflected light.

B. Measurement Principle

The polarized light irradiating the grating lines produces different diffraction waveforms for different sample conditions. The waveform depends on the dimensions of the pattern profile (pitch, linewidth, sidewall angle, etc.), the optical characteristic of material that constitutes the pattern, the slope angle of the grating, the polarization direction of the incident light, and the angle of incidence. The measurement system uses the incident angle light for target pattern and detects light of only the zeroth-order diffraction. The system provides light under two conditions with regard to the angle between polarization direction and the direction of the grating lines: 0° (TM) and 90° (TE). If the optical characteristics of the grating material are uniform, the waveform of zeroth-order diffraction is determined by the pattern profile. The pattern profile can therefore be obtained by analyzing the diffraction waveform. We have done this by using rigorous coupling wave analysis (RCWA) methods [5]. Fig. 4 shows examples of the waveforms the system obtained in the TE and TM modes.

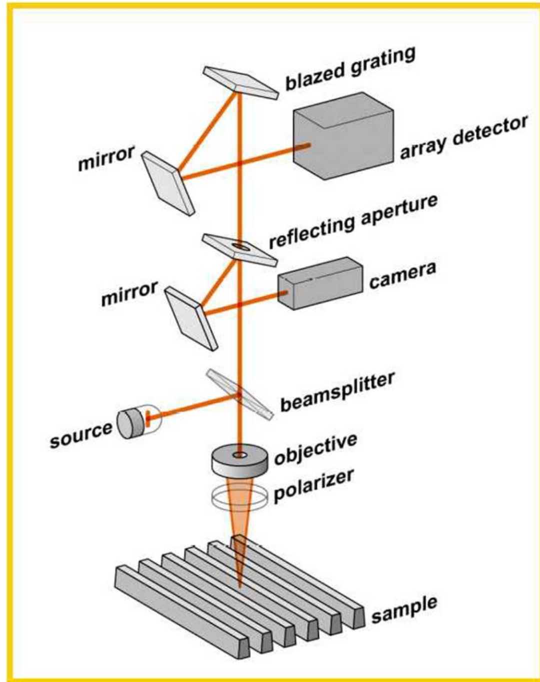

Fig. 3. System configuration.

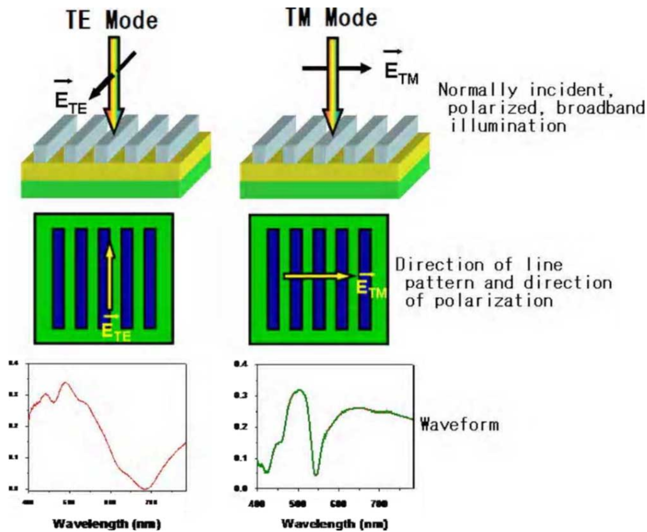

Fig. 4. Polarization modes and examples of corresponding waveforms.

C. Waveform Analysis Method

It is very difficult to describe the pattern profile change by the function because it changes into complexity. The profile is therefore divided into multiple shapes at the inflection points of its characteristics, and models are created by combining two or more trapezoids as shown in Fig. 5.

Each trapezoid is then subdivided into rectangles and the model waveform is calculated by RCWA methods. To obtain the actual pattern profile, we need to evaluate the fitting of the model to the measurement results. The best fitting model shape is regarded as the actual pattern profile. Fig. 6 shows the analysis flow of the model fitting. The parameters of the pattern model are the critical dimensions of each part of the trapezoid (bottom CD, top CD, sidewall angle, and thickness) and the thickness of the pattern substrate.

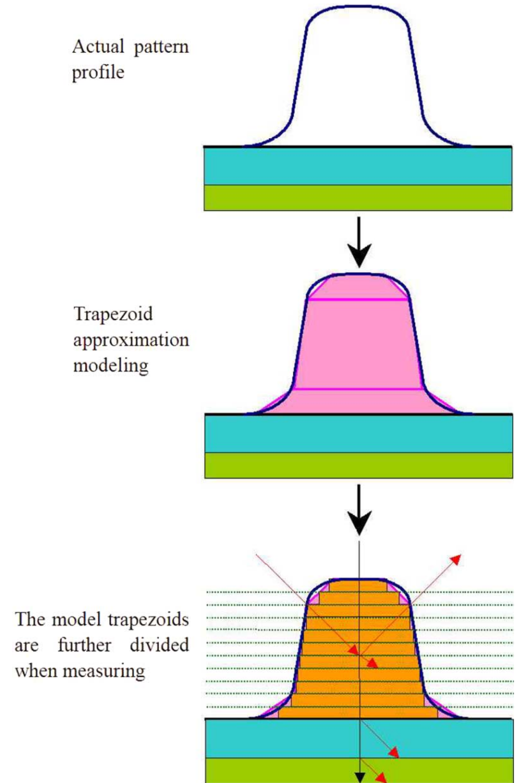

Fig. 5. Modeling grating pattern and subdividing model.

D. Evaluation of Measurement Validity (Fitting)

The accuracy of the pattern model is evaluated by measuring the fitting of the modeled waveform to the measured waveform. This is done using the mean squared error (MSE) given by the following equation:

$$\mathrm{MSE} = \frac{1}{N-M}\sum_{\mathrm{i}=1}^{N}\left(\frac{\mathrm{R}_i^{\mathrm{Model}} - R_i^{\mathrm{Experimental}}}{\sigma_i}\right)^2 \tag{2}$$

where N is the number of reflectivity data, M is the number of fitting parameters in the model, and σ_i is the standard deviation of R data at the several times measurement results. The data obtained in five measurements is used in this calculation. The MSE is smaller when the fitting is better and is zero when the fitting is perfect. Generally, goodness-of-fit (GOF) is used as an index of the fitting. It is related to the MSE as follows:

$$\mathrm{GOF} = \mathrm{Exp}\left(\frac{-\mathrm{MSE}}{s}\right) \tag{3}$$

where s is a constant scale factor.

E. Modeling

1) Feature of Change in Measurement Waveform by Focus Change: Reflectance spectra obtained with the TE and TM polarizations at various focus offsets are shown in Fig. 7(a) and

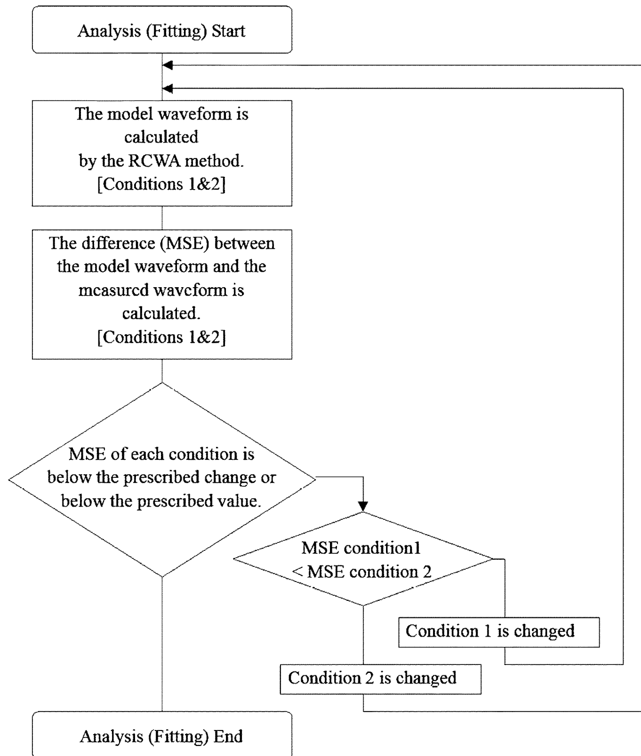

Fig. 6. Analysis flow.

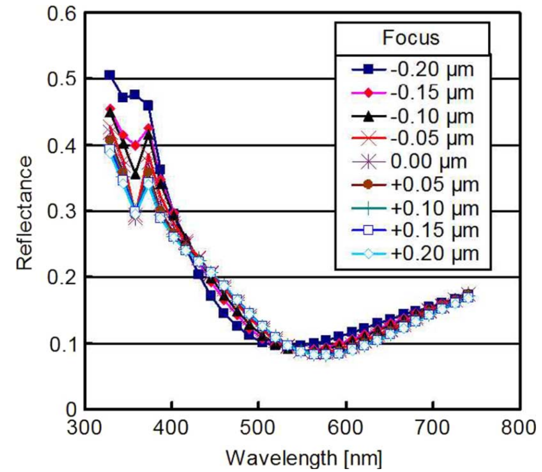

(a)

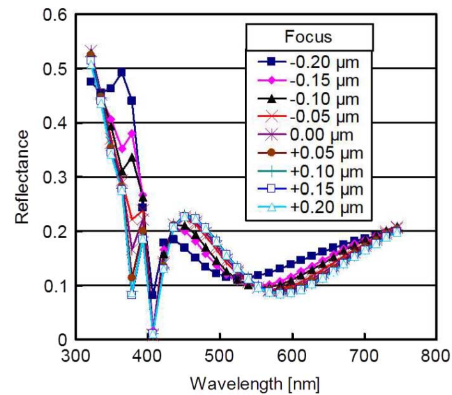

(b)

Fig. 7(a). Spectrum curve at each focus offset: (a) TE mode and (b) TM mode.

7(b). Because the variation of the PR profile was small, no significant shift of peak locations is evident.

Our analysis of the PR profile must therefore be based on minute variances of the measured waveform if we are to improve the fitting between the measured and modeled waveforms. To do this, we need a model that faithfully reflects the change of PR profile.

2) Modeling of PR Profile: PR profile characteristics for model creation were extracted from cross-sectional SEM images like those shown in Fig. 2. These PR profiles showed such characteristics as a smaller width in the central part of the sidewall, rounding of the upper part, footing at the bottom edge, etc. The corresponding PR profile model is shown in Fig. 8.

The lines in part (a) of Fig. 8 show a two-layer PR model reflecting the smaller width in the central part of the sidewall, and those in (b) show a three-layer version, additionally reflecting the rounding of the upper part. The rounded shape is calculated by the half width of the difference between the top and bottom parts with the thickness at the target layer. The rounded layer shows good fitting with the X-SEM profile. Fig. 8(c) shows a four-layer model made by putting a footing at the bottom edge, and (d) shows a five-layer model as optimization of the pattern shape at the upper rounded area.

F. Evaluation of Validity of Model

A multilayer model approximates the actual PR cross section well, but instead we need to use an optimized model because the analysis time increases with the number of layers. We evaluated the fitting performance of each model shown in Fig. 8 and selected for this analysis the best model providing the required accuracy.

Model accuracy is also influenced by the optical characteristics of each layer, and these vary depending on the conditions of the film-forming process. Therefore, the film sample was made by the same process as measurement model pattern for each layer's optical characteristics analysis. A spectroscopic reflectometer (SR) and a spectroscopic ellipsometer (SE) were used for this measurement.

1) Validity of Model Analysis Result: The CD size change (i.e., PR profile variation) due to focus fluctuation is shown in Fig. 9 for each model. The PR profile sometimes shows unexpected fluctuation at the case of two-layer and three-layer models, so models with four or more layers have to be used. In addition, the thicknesses of nongrating (substrate) layers are float parameters and are the fitting estimate of this part. The substrate layer thicknesses measured under various focus conditions are shown in Fig. 10. The four-layer model shows a discontinuous thickness change at the focus position of -0.1 μm. We judged from these analysis results that a five-layer model is needed to guarantee the measurement accuracy.

2) MSE: Fig. 11 shows the waveform fitting evaluation results of each model at the best focus PR profile that uses ten wafers. It is possible to judge the quality of each model's fitting and PR profile repeatability by this method. The MSE value gets close to converging in the four-layer model. The MSE change

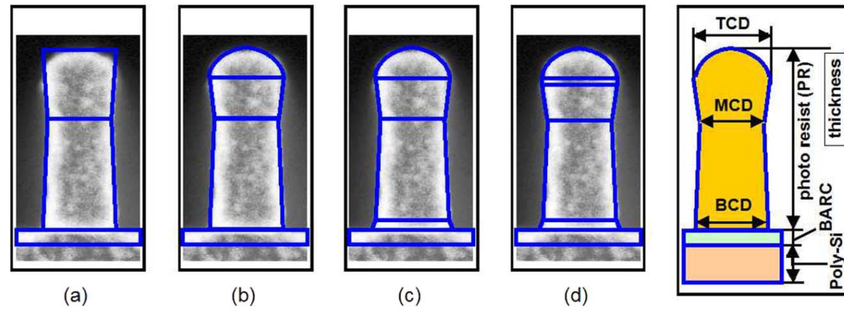

Fig. 8. Cross-sectional SEM profiles and model of those profiles.

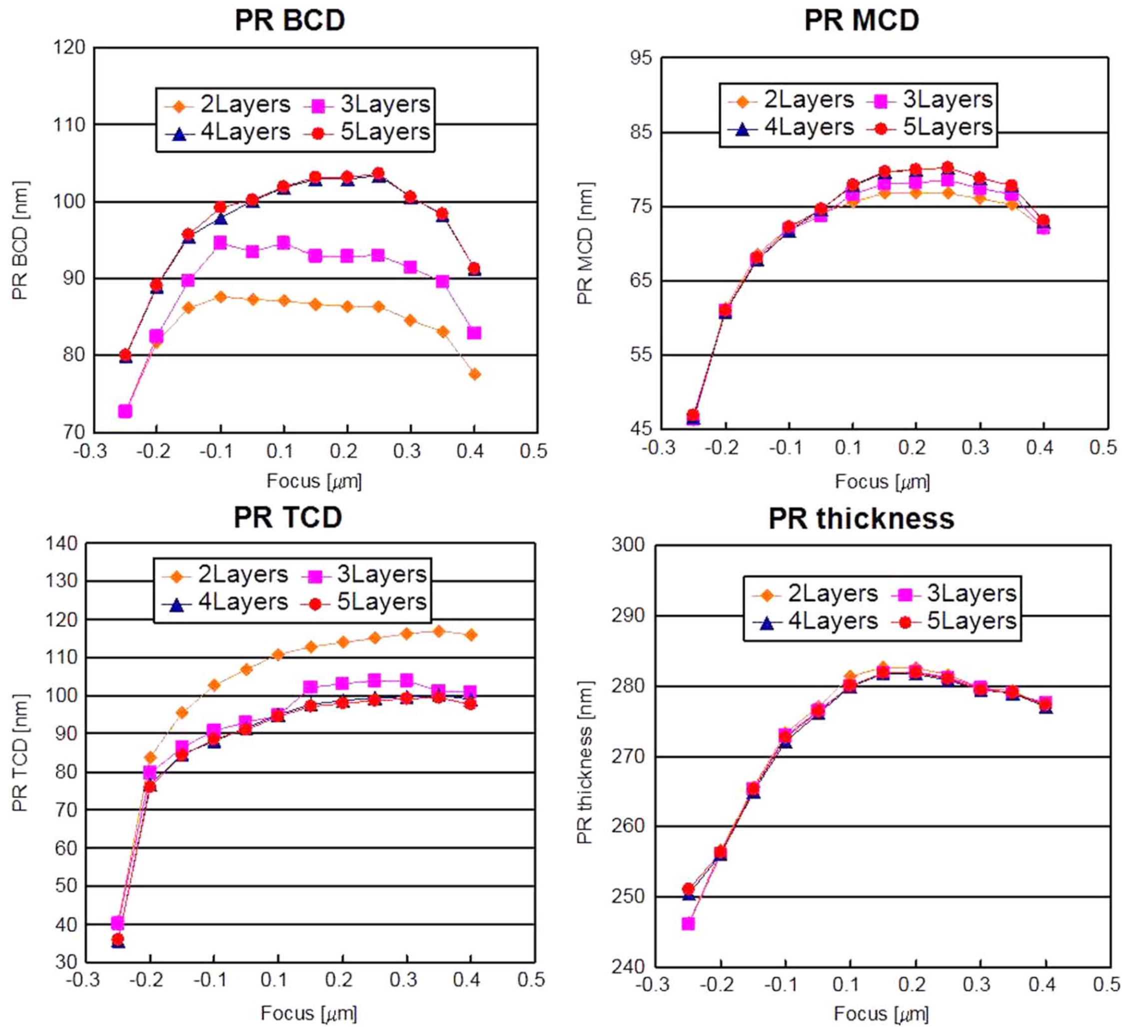

Fig. 9. PR size change due to focus fluctuation.

due to focus fluctuation is shown in Fig. 12 for each model. The MSE for the four-layer model increases at the focus position of -0.15 μm, but the MSE for the five-layer model does not. We therefore decided to use the five-layer model.

The MSE results obtained using the five-layer model at all points on the surface of an FEM wafer are shown in Fig. 13. MSE values less than seven were obtained in most areas (i.e., under most conditions), except for the extreme defocus and deviate exposure dose areas from FEM wafer. Especially, critical exposure dose and focus areas show small MSE values as less than four.

We judged from these evaluation results that the five-layer model yields sufficient measurement accuracy with our new technique, and this model was used in the following analysis.

G. Application Model

We developed a PR profile scatterometry model with eight layers: five layers of PR and three layers of unpatterned films (Fig. 14). Each layer was characterized by thickness, linewidth (LW), and sidewall angle (SWA). The layers from L4 to L8 show the characteristics of PR profile at each position. L4 corresponds

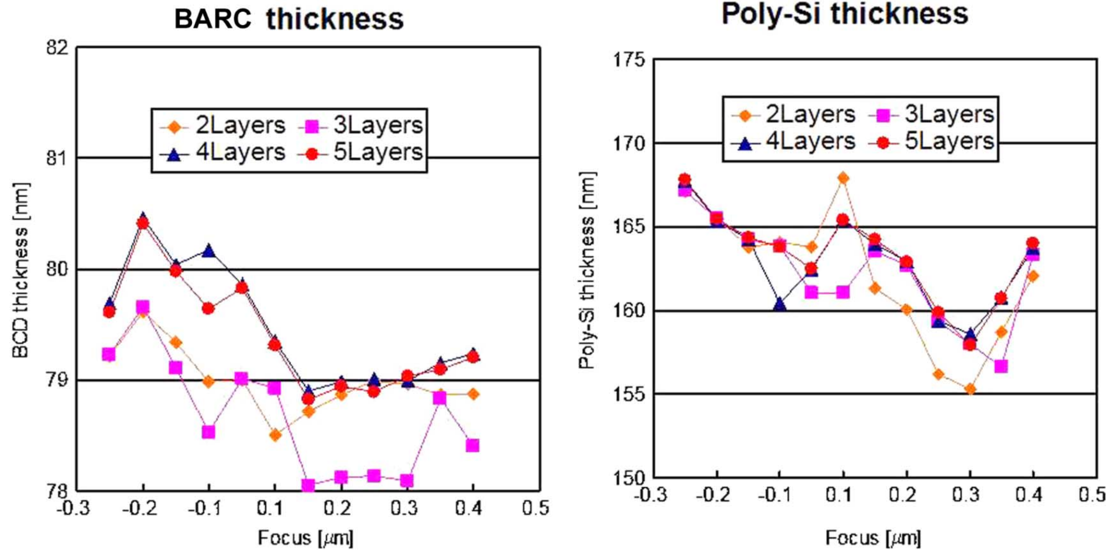

Fig. 10. Substrate layer thickness change due to focus fluctuation.

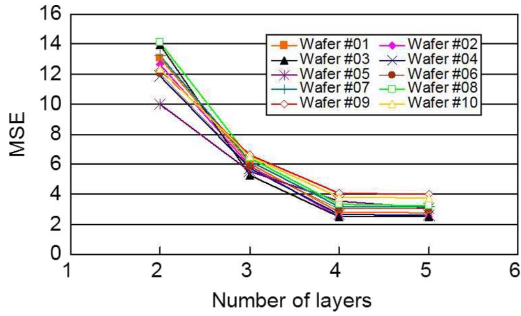

Fig. 11. MSE changes of each model.

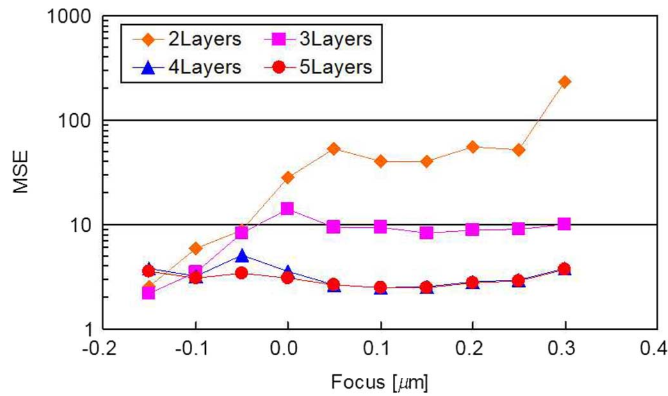

Fig. 12. MSE changes due to focus fluctuation.

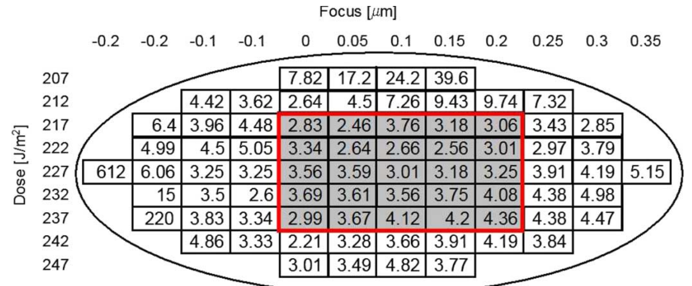

Fig. 13. MSE results obtained on FEM wafer.

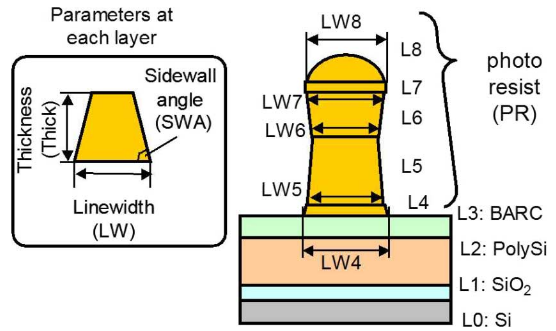

Fig. 14. Scatterometry model for focus monitoring.

to the PR footing in the bottom area. L5 and L6 model the tapered shape of the middle area, and L8 models the round top of the PR. L7 is an additional factor for the PR top shape, and it improves the accuracy at the model fitting.

We derived focus values from the experimental data by using the multiple regression method.

H. Accuracy of Measurement Model

We evaluated the accuracy of the measurement model by comparing the results of scatterometry measurements with those obtained using other inspection tools. The values of the PR pattern width obtained by scatterometry are compared with X-SEM observations in Fig. 15(a) and (b). The square of the correlation coefficient is 0.765 for LW6 (linewidth at the bottom of layer 6) and is 0.937 for LW7. We thus find good correlation between scatterometry measurements and X-SEM measurements.

III. EXPERIMENTAL RESULTS

Focus values were calculated using a formula that is based on the results of our scatterometry measurements. Table II summarizes a parameter setting of each layer in the resist pattern mea-

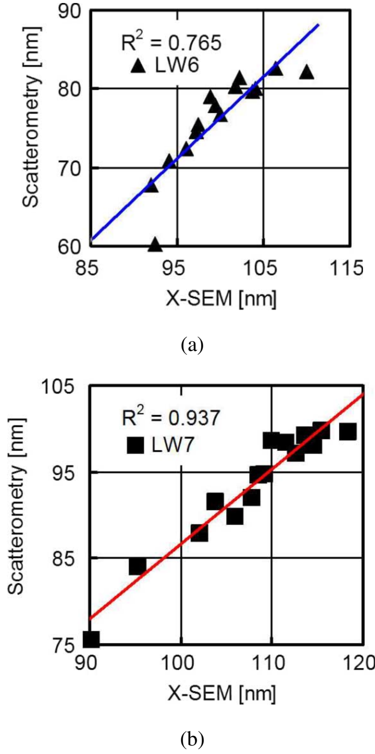

Fig. 15. (a) LW6 values obtained by scatterometry versus those obtained by X-SEM. (b) LW7 values obtained by scatterometry versus those obtained by X-SEM.

TABLE II
SETTING OF MEASUREMENT PARAMETERS

Layer No.	Material	Thick	SWA	LW
L8	PR	Float	Float	Link
L7	PR	Fix	Fix	Link
L6	PR	Float	Float	Link
L5	PR	Fix	Float	Link
L4	PR	Fix	Fix	Float
L3	BARC	Float	-	-
L2	Poly-Si	Float	-	-
L1	SiO_2	Float	-	-
L0	Si	-	-	-

surement model shown in Fig. 14. Each layer is defined by the measurement parameter of thickness (Thick), linewidth (LW), and a sidewall angle (SWA). The measurement target parameters are set as variable (float) values and the parameters with a small change are set as fixed (fix) values. Furthermore, the parameters that interlock with each other and change between the continuous layers are set as the linkage value (link), such as the linewidth between the L5 upper part and L6 bottom part.

A. *Evaluation of Focus Prediction Formula by Multiple Linear Regression (MLR)*

A focus value is predicted from the measurement result of scatterometry with deriving the multiple linear regression models

$$\hat{y} = \beta_0 + \beta_1 x_1 + \beta_2 x_2 + \cdots + \beta_p x_p \tag{4}$$

TABLE III
MATRIX OF FOCUS CONDITION AND MEASUREMENT RESULT

No.	Focus setting	Meas. result 1	Meas. result 2	...	Meas. result p
1	y_1	x_{11}	x_{21}	...	x_{p1}
2	y_2	x_{12}	x_{22}	...	x_{p2}
3	y_3	x_{13}	x_{23}	...	x_{p3}
⋮	⋮	⋮	⋮	⋮	⋮
n	y_n	x_{1n}	x_{2n}	...	x_{pn}

where $\hat{y}$ is the objective variable that means a focus values. $x_1 \sim x_p$ is an explanatory variable that means each measurement parameter of scatterometry, such as thickness, sidewall angle, and linewidth. Moreover, β is a regression coefficient. The focus prediction formula is formulized from deriving the β using the measurement result of the FEM wafer, as shown in Fig. 13.

The focus setting of the aligner equipment is listed in Table III along with the corresponding measurement results. The error ε_{j} is the difference between the objective variable $\hat{y}_{\mathrm{j}}$ and the actual focus setting y_{j}

$$\varepsilon_{\mathrm{j}} = y_{\mathrm{j}} - \hat{y}_{\mathrm{j}}. \tag{5}$$

MLR calculates the regression coefficient β that minimalizes the squared sum of error values $\sum_{j=1}^{n} \varepsilon_{\mathrm{j}}^2$ in the setting range of 1 to n [6]. When an explanatory variable has correlation, the accuracy of regression degrades in the MLR methods. Then, the focus prediction formula was calculated only using the float parameters as shown in Table II and applied for the measurement results of 0.0–0.2 μm in focus range and dose range of 217–237 J/m^2

$$\begin{aligned}\text{Focus} = {} & 0.025249 + 0.063028 \times \text{LW4} + 0.006355 \\ & \times \text{SWA5} + 0.040848 \times \text{Thick6} \\ & - 0.007809 \times \text{SWA6} \\ & - 9.902141 \times \text{Thick8}\end{aligned} \tag{6}$$

where Thick is the thickness (in nanometers), LW is the linewidth (in nanometers), and SWA is the sidewall angle (in degrees). Fig. 16 shows the focus measurement results calculated by prediction (6). Focus measurement shots are in the 0.0–0.2 μm focus range and dose range of 217–237 J/m^2 at four FEM wafers that exposed by Fig. 13 conditions. These are the same wafers as used for deriving (6). The plotted points are the average focus values and the error bar means the raw data of the four wafers of each measurement result. The focus measurement accuracy shows $\pm$40-nm variation. However, the systematic error had arisen in the focus prediction result, and inclination and offset of the fitting line between the measurement value and a setting focus value were, respectively, 0.805 and 26 nm. The multicollinearity between each parameter is a reason for generating the systematic error at the PR profile changes even if we formulize the focus prediction only with float parameters. To predict a focus value with practical accuracy, we need to formulize it with the correlation between each parameter undisturbed. Zero systematic error is an ideal target.

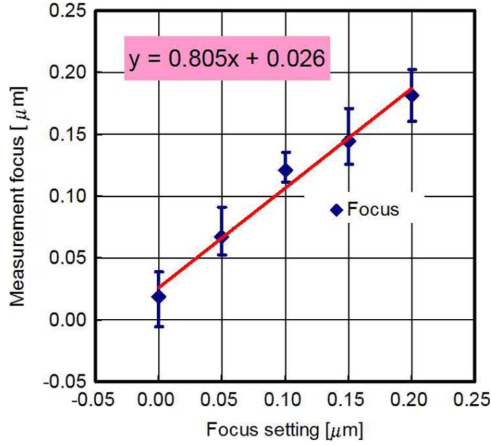

Fig. 16. Focus measurement results estimated by MLR.

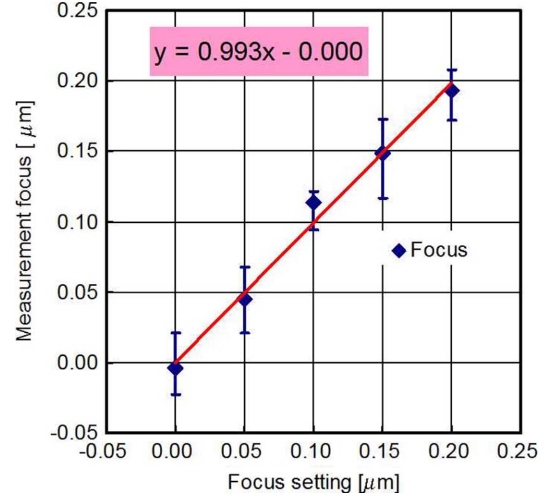

Fig. 17. Focus measurement results estimated by PLS.

The change rate of measurement values to setting values of the focus shows the inclination 1 and offset 0 in this case.

B. *Evaluation of Focus Prediction Formula by Partial Least Squares Regression (PLS)*

Partial least squares regression derives the regression formula excluding the effect of multicollinearity by not executing direct regression from the measurement results X_{ij} but intervening in the latent variables. It can therefore derive regression formulas with sufficient accuracy even when an explanatory variable X has a correlation

$$\begin{aligned} T_{i1} &= c_{11}x_{i1} + c_{12}x_{i2} + \cdots + c_{1p}x_{ip} \\ T_{i2} &= c_{21}x_{i1} + c_{22}x_{i2} + \cdots + c_{2p}x_{2p} \end{aligned} \tag{7}$$

where T means the latent variable. The coefficient C_{1j} is fixed to maximize the covariance between T_1 and y at the PLS methods. T_2 is an uncorrelated part with T_1 and coefficient C_{2j} is fixed to maximize the covariance between T_2 and y. The focus estimation value is showed by (8), and it is possible to extract it by calculating the regression coefficient β [6]

$$\hat{y}_j = \beta_0 + \beta_1 T_{1j} + \beta_2 T_{2j}. \tag{8}$$

The focus prediction formula was formulized based on float and the link parameters which are shown in Table II by using the PLS methods

$$\begin{aligned} \text{Focus} = {} & 156.240350 - 0.138259 \times \text{LW4} - 0.724563 \\ & \times \text{SWA5} - 0.081151 \times \text{Thick6} \\ & - 0.253507 \times \text{LW6} \\ & - 0.901823 \times \text{SWA6} - 0.358433 \\ & \times \text{LW7} + 0.131232 \\ & \times \text{Thick8} - 0.112873 \times \text{SWA8} \end{aligned} \tag{9}$$

where Thick is the thickness (in nanometers), LW is the linewidth (in nanometers), and SWA is the sidewall angle (in degrees). Fig. 17 shows the focus measurement result calculated by the prediction (9). Focus measurement shots are in the 0.0–0.2 μm focus range and dose range of 217–237 J/m^2 at four FEM wafers that exposed by Fig. 13 conditions. These are the same wafers as used for deriving (9). The plotted points are the average focus values and the error bar means the raw data of the four wafers of each measurement result. The focus measurement accuracy shows ±30 nm variation. The systematic error in the focus prediction result is very small, and inclination and offset of the fitting line through the measured and set focus values were, respectively, 0.993 and 0 nm. PLS methods thus yield a smaller systematic error than the MLR methods do. We consider this to achieve the formulization without disturbing the correlation between each parameter by applying the PLS methods.

Focus can be calculated, with practical accuracy, by using the multiple regression model based on scatterometry measurement results. This formula uses linear expression that is easily calculated by scatterometry equipment function. We can use an on-board reporting system for focus calculation. It is a great advantage for workload reduction of FA systems.

C. *Focus Measurement Results*

PR profile variation in actual production wafers is caused by not only focus fluctuation but also exposure dose shifting. We have to pick up a focus component from this total PR profile fluctuation. Of course, focus measurement needs a guarantee of accuracy at wide focus range. We confirmed the accuracy of our new measurement technique as shown in Fig. 17. We measured four FEM production wafers with exposure dose variation of 10 J/m^2 and focus offset variation of 0.1 μm as shown in Fig. 13. These conditions assume the situation of production lot processing. As shown in the foregoing paragraph, the focus measurement accuracy shows ±30 nm variation and a very small systematic error. Fig. 17 includes the exposure dose variation of 10 J/m^2 but focus measurement result shows high accuracy. This means that we can exclude the exposure-dose-shifting effect from the focus measurement. This result shows that the new technique achieved high-accuracy nondestructive focus measurement on the production wafers.

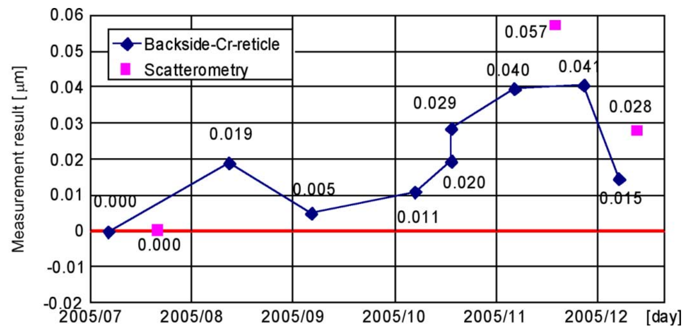

Fig. 18. Trend of focus measurements by scatterometry and backside-Cr-reticle method [7].

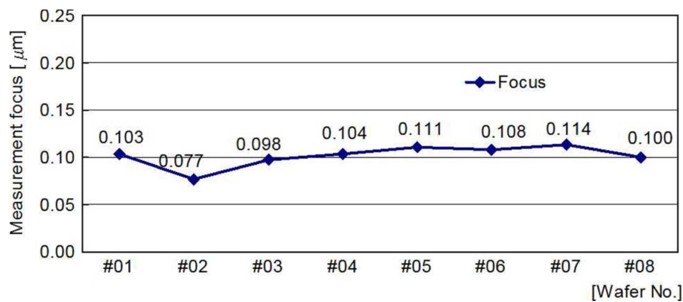

Fig. 19. Focus fluctuation measured in one lot.

In the periodic correction of the focus offset of aligner equipment, we are using the backside-Cr-reticle method [7]. This method uses a special reticle with dedicated wafers. It has to stop the aligner during exposing the dedicated wafer. From the point of view of the aligner machine time, we cannot improve a measurement frequency. Fig. 18 shows the trend focus-check results obtained using the backside-Cr-reticle method. The focus values of production wafers obtained using our method show good correlation with those obtained using the backside-Cr-reticle method.

The current method can be replaced by our new one. We can correct the focus offset more frequently without increasing the aligner machine downtime. This will reduce the required-DOF due to aligner fluctuation. We can get sufficient focus margins for mass production of even the most advanced devices. Run-to-run focus measurement is an effective method for increasing the repeatability of the PR shape, and Fig. 19 shows the measurement results for eight wafers picked out of a normal exposed production lot.

The small focus fluctuation, ranging over only 37 nm, assures good focus stability in this lot. PR shape repeatability can be improved by reworking defocused wafers when abnormal focus value is detected.

D. In the Future

This focus measurement method is useful for further improvement of the PR shape repeatability. We confirmed that the new technique has good measurement accuracy from each evaluation. Repeatability of the PR shape including CD depends on the fluctuation of both focus and exposure dose. So far, exposure dose is corrected by feedback of CD measurement. We can introduce a feedback method of the focus with this measurement method. The feedback of both focus and exposure dose enables us to achieve better repeatability of PR shape that ensures better stability of final pattern after etching.

IV. Conclusion

We have succeeded in extracting parameters characterizing small focus-dependent variations of PR profile by using scatterometry. PR profile characteristics used for model creation were extracted from X-SEM images. Among these characteristics were smaller widths in the central part of the sidewall, rounding of the upper part, and footing at the bottom edge. We evaluated the fitting performance of several PR profile models representing these characteristics and selected the best one providing the required accuracy. We then developed an eight-layer model assuring profile faithfulness, substrate-layer-thickness accuracy, and MSE. This scatterometry model includes five layers of PR and three layers of unpatterned substrate films. Focus is calculated from scatterometry measurement results by using a PLS formula because PLS methods yielded a smaller systematic error than MLR methods did. We developed a formula that is not influenced by correlation between measurements. Our new focus-monitoring method enables us to measure the focus of production wafers. Measurement results and setting values show good correlation (i.e., are within 30 nm) at the focus variation of 0.1 μm. The new method makes it possible to increase the frequency of focus offset correction without increasing aligner machine downtime. This change will reduce the required-DOF due to aligner fluctuation and will enable us to get sufficient focus margins for mass production of devices beyond the 90/65 nm node devices. Feedback of focus values obtained by this method will help providing precise CD control for most advanced device applications.

Acknowledgment

The authors would like to thank the researchers at Hitachi, Ltd., and Nanometrics Japan, Ltd., for their scatterometry tools and analysis applications.

References

[1] *ITRS*, 2006 update, 2006, Lithography.
[2] E. Fisch, "Aids for driving lithography hard: Wafer level process control features," *Proc. SPIE*, vol. 4346, pp. 1003–1010, 2001.
[3] M. Aasano, "Run-to-run CD error analysis and control with monitoring of effective dose and focus," *Proc. SPIE*, vol. 5038, pp. 239–246, 2003.
[4] B. Eichelberger, "Simultaneous dose and focus monitoring on product wafers," *Proc. SPIE*, vol. 5038, pp. 247–254, 2003.
[5] M. G. Moharam and T. K. Gaylord, "Rigorous coupled-wave analysis of planar-grating diffraction," *J. Opt. Soc. Amer.*, vol. 71, pp. 811–818, 1981.
[6] I. E. Frank and J. H. Friedman, "A statistical view of some chemometrics regression tools," *Technometrics*, vol. 35, no. 2, pp. 109–135, 1993.
[7] S. Nakao *et al.*, "Simple and high sensitive focus monitoring utilizing an aperture on backside of photomask," *Proc. SPIE*, vol. 5040, pp. 582–589, 2003.

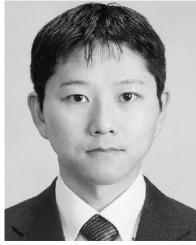

Toshihide Kawachi received the B.S. and M.S. degrees in electric engineering from Musashi Institute of Technology, Tokyo, Japan, in 1993 and 1995, respectively.

He joined Mitsubishi Electric Corporation in 1995. Since then, he has been responsible for lithography process development and productivity improvement. From 2000 to 2003, he joined Mitsubishi Semiconductor Europe GmbH, Germany. He is currently an Engineer of Renesas Technology Corporation, Ibaraki, Japan. His research interests include metrology system for semiconductor manufacturing, equipment engineering system, and process control systems.

Hidekimi Fudo joined Hitachi , Limited, in 1991. He has worked on the Electron Beam Direct Writing Technology Section. Since 2000, he has worked on lithography process development. He is currently an Engineer of Renesas Technology Corporation, Ibaraki, Japan. His research interests include metrology system for semiconductor manufacturing, lithography process development, and productivity improvement. Specifically, he is working on the development for scatterometry applications.

Yoshio Iwata received the B.S. and M.S. degrees in precision engineering from Kyoto University, Kyoto, Japan, in 1988 and 1990, respectively. He received the Ph.D. degree in engineering from Osaka University, Osaka, Japan, in 2003.

He joined the Production Engineering Research Laboratory, Hitachi, Limited, in 1990. From 1999 to 2000, he was a Visiting Scholar at Stanford University, Stanford, CA. He is currently a Group Manager of Renesas Technology Corporation, Ibaraki, Japan. His research interests include equipment engineering system, quality control systems, and process control systems.

Shunichi Matsumoto received B.S. and M.S. degrees in mechanical engineering from Tokyo Institute of Technology, Tokyo, Japan, in 1989 and 1991, respectively.

Since 1991, he has been with Hitachi Production Engineering Research Laboratory and he has worked on R&D for inspection systems of electronics products. He is currently a Senior Researcher in the Image Recognition and Inspection System Department and working on optical metrology system for semiconductor manufacturing.

Hideaki Sasazawa received the B.S. and M.S. degrees in electrical engineering from Chuo University, Tokyo, Japan, in 1991 and 1993, respectively.

He joined Hitachi, Limited, in 1993. Since then, he has worked on R&D for inspection systems of electronics products. He worked on the research for the scatterometry application of semiconductor manufacturing from 2003 to 2005. Currently, he is a Senior Researcher of the Image Recognition and Inspection System Department of Production Engineering Research Laboratory, Kanagawa, Japan.

Tadayoshi Mori received the M.S. degree in chemistry in the field of the gas–solid surface chemistry from Rikkyo University, Japan, in 1986.

He is an Application Engineer of Nanometrics Japan, Limited, Tokyo. He has the experience of 21 years in the field of a micro lithography and optical CD technology.